Inorg. Chem. **2007**, *46*, 3548–3556

Distinct M and P Helical Complexes of H_2O and Metal Ions Ni^{II}, Cu^{II}, and Zn^{II} with Enantiomerically Pure Chiral Bis(pyrrol-2-ylmethyleneamine)cyclohexane Ligands: Crystal Structures and Circular Dichroism Properties

Yaobing Wang,[†,‡] Hongbing Fu,*[,†] Fugang Shen,[†,‡] Xiaohai Sheng,[†,‡] Aidong Peng,[†] Zhanjun Gu,[†,‡] Hongwei Ma, Jin Shi Ma,[†] and Jiannian Yao*[,†]

Beijing National Laboratory for Molecular Sciences, Institute of Chemistry, Chinese Academy of Sciences, Beijing 100080, People's Republic of China, and Graduate School, Chinese Academy of Sciences, Beijing 100039, People's Republic of China

Received December 5, 2006

The enantiomerically pure bis-bidentate ligands of bis(pyrrol-2-ylmethyleneamine)cyclohexane [$H_2(L^{R,S})$] are easily synthesized from condensation of the pure *R*,*R* and *S*,*S* enantiomers of the 1,2-diaminecyclohexane spacer with 2 equiv of pyrrole-2-carbaldehyde. The coordination of [$H_2(L^{R,S})$] with a H_2O molecule and metal ions Ni^{II}, Cu^{II}, and Zn^{II} gives rise to distinct helical structures and crystal packing motifs: homochiral and enantiopure infinite single-helical polymeric chains of [$(H_2(L^{R,S})\cdot H_2O)_n$] via hydrogen bonds, mononuclear single helices of [$Ni^{II}(L^{R,S})$] and [$Cu^{II}(L^{R,S})$], and a double-stranded dinuclear helicate of [$Zn^{II}_2(L^{R,S})_2$], respectively. The helical structures for all metal complexes in the solid state still remain in the solution. Remarkably, chiral ligands of [$H_2(L^R)$] and [$H_2(L^S)$] predetermine the chirality of the helices and helicates, i.e., P left-handedness and M right-handedness, respectively. The structural changes of these complexes induced by different coordinators are also characterized by circular dichroism (CD) and absorption spectra in both the solid state and solution. Analysis of CD spectra, with aids of absolute determination of single-crystal X-ray diffraction structures, reveals both intraligand and interligand chromophore couplings. For the potential applications of these complexes, other experiments such as magnetism, photoluminescence, and nonlinear optical properties have also been investigated.

Introduction

Chirality is one of the important aspects to fields as diverse as asymmetric catalysis,[1] bioinorganic chemistry,[2] and supramolecular chemistry.[3] The enantioselective synthesis of pure P or M helical structures by coordination of the ligand, especially the chiral ligands, with labile metal cations has been studied with great interest over the last decades.[4−9] Of the factors integral to helical structure formation, the geometric preferences of the metal and the spacer that separates and links the donor atoms of the ligands are

* To whom correspondence should be addressed. E-mail: hongbing.fu@iccas.ac.cn (H.F.), jnyao@iccas.ac.cn (J.Y.). Tel/Fax: 86-10-82616517.

† Beijing National Laboratory for Molecular Sciences, Institute of Chemistry.

‡ Graduate School.

(1) (a) Fu, G. C. *Acc. Chem. Res.* **2006**, *39*, 853−860. (b) Inanaga, J.; Furuno, H.; Hayano, T. *Chem. Rev.* **2002**, *102*, 2211−2226. (c) Chelucci, G.; Thummel, R. P. *Chem. Rev.* **2002**, *102*, 3129−3170. (d) Bennani, Y. L.; Hanessian, S. *Chem. Rev.* **1997**, *97*, 3161−3196. (e) Ramón, G. A.; Javier, A.; Juan, C. C. *Angew. Chem., Int. Ed.* **2006**, *45*, 7674−7715. (f) Jens, H.; Simone, D.; Marco, G.; Philipp, S.; Ingrid, S.; Hartmut, F.; Alexander, M.; Dietmar, S. *Eur. J. Org. Chem.* **2003**, *13*, 2388−2408. (g) Katsuki, T. *Chem. Soc. Rev.* **2004**, 437−444. (h) Laetitia, C.; David, C. S. *Chem. Soc. Rev.* **1999**, *2*, 85−93.

(2) (a) von Herausgegeben, S. J. L. Progress in Inorganic Chemistry. *Bioinorganic Chemistry*; Wiley: New York, 1990; Vol. 38. (b) von Herausgegeben, J. R. L. *The Bioinorganic Chemistry of Nickel*; VCH Verlagsgesellschaft: Weinheim, Germany, 1988. (c) Szacilowski, K.; Macyk, W.; Drzewiecka-Matuszek, A.; Brindell, M.; Stochel, G. *Chem. Rev.* **2005**, *105*, 2647−2694. (d) Wilson, L.; Pollard, A. M. *Acc. Chem. Res.* **2002**, *35*, 644−651. (e) Philip, M. *Chem. Soc. Rev.* **1998**, *2*, 105−116.

(3) (a) Lehn, J.-M. Concepts and Perspectives. *Supramolecular Chemistry*: VCH: Weinheim, Germany, 1995. (b) Kaes, C.; Katz, A.; Hosseini, M. W. *Chem. Rev.* **2000**, *100*, 3553−3590. (c) Seidel, S. R.; Stang, P. J. *Acc. Chem. Res.* **2002**, *35*, 972−983. (d) Stang, P. J.; Olenyuk, B. *Acc. Chem. Res.* **1997**, *30*, 502−518. (e) Leininger, S.; Olenyuk, B.; Stang, P. J. *Chem. Rev.* **2000**, *100*, 853−908. (f) Fujita, M. *Acc. Chem. Res.* **1999**, *32*, 53−61. (g) Fujita, M.; Tominaga, M.; Hori, A.; Therrien, B. *Acc. Chem. Res.* **2005**, *38*, 369−378. (h) Bunzli, J.-C. G.; Piguet, C. *Chem. Rev.* **2002**, *102*, 1897−1928. (i) Piguet, C.; Bernardinelli, G.; Hopfgartner, G. *Chem. Rev.* **1997**, *97*, 2005−2062.

10.1021/ic062316z CCC: $37.00
Published on Web 03/30/2007

particular influential.[10−12] Despite the ongoing researches into helical structures, few examples exist of neutral compounds that adopt helical structures.[13−16]

Most recently, we demonstrated that pyrrol-2-yl Schiff base ligands serve as ideal building blocks for supramolecular architectures. By variation of the spacers between two pyrrolimine units or the substituents on the pyrrole ring, multidimensional network polymers, dinuclear dimeric helicates, and trinuclear trimeric triangle and tetranuclear tetrameric square complexes were generated.[17] Potential applications, such as sensors, were also investigated.[18] In fact, the building blocks also exhibit unique character, such as facile synthesis and uncharged complexes that are easy to purify and crystallize.

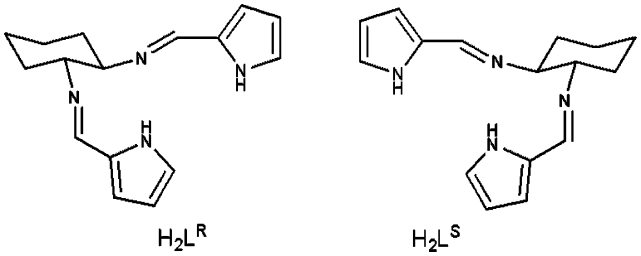

Figure 1. Structures of $H_2(L^R)$ (left) and $H_2(L^S)$ (right) ligands.

In this report, chiral ligands $[H_2(L^R)]$ and $[H_2(L^S)]$ (Figure 1) are easily synthesized from condensation of the pure (*R*,*R*)- and (*S*,*S*)-1,2-diaminecyclohexane spacers with 2 equiv of pyrrole-2-carbaldehyde. We found that the coordination of $[H_2(L^{R,S})]$ with a H_2O molecule and different metal ions Ni^{II}, Cu^{II}, and Zn^{II} gives rise to distinct molecular structures and crystal packing motifs. The structural changes of these complexes induced by different coordinators are also characterized by circular dichroism (CD) and absorption spectra in both the solid state and solution. For the potential applications of these chiral complexes, experiments on magnetism, photoluminescence, and nonlinear optical (NLO) properties have also been investigated.

Experimental Section

All starting materials were purchased from Aldrich and used without further purification. Melting points were determined with a Yanaco MP-500 micro melting point apparatus. The thermo-

(4) (a) Quinodoz, B.; Labat, G.; Stoeckli-Evans, H.; von Zelewsky, A. *Inorg. Chem.* **2004**, *43*, 7994−8004. (b) Glasbeek, M.; Sitters, R.; van Veldhoven, E.; von Zelewsky, A.; Humbs, W.; Yersin, H. *Inorg. Chem.* **1998**, *37*, 5159−5163. (c) Bark, T.; Zelewsky, A.; Rappoport, D.; Neuburger, M.; Schaffner, S.; Lacour, J.; Jodry, J. *Eur. J. Inorg. Chem.* **2001**, *5*, 1207−1220. (d) Kolp, B.; Abeln, D.; Stoeckli-Evans, H.; Zelewsky, A.; Hamann, C. *Dalton Trans.* **2004**, *3*, 402−406.

(5) (a) Hannon, M. J. *Chem. Soc. Rev.* **2007**, *2*, 280−295. (b) Pascu, M.; Clarkson, G. J.; Kariuki, B. M.; Hannon, M. J. *Dalton Trans.* **2006**, *22*, 2635−2642. (c) Hannon, M. J.; Meistermann, I.; Isaac, C. J.; Blomme, C.; Aldrich-Wright, J. R.; Rodger, A. *Chem. Commun.* **2001**, *12*, 1078−1079. (d) Hotze, A. C. G.; Kariuki, B. M.; Hannon, M. J. *Angew. Chem., Int. Ed.* **2006**, *45*, 4839−4842. (e) Childs, L. J.; Malina, J.; Rolfsnes, B. E.; Pascu, M.; Prieto, M. J.; Broome, M. J.; Rodger, P. M.; Sletten, E.; Moreno, V.; Rodger, A.; Hannon, M. J. *Chem.*−*Eur. J.* **2006**, *12*, 4919−4927. (f) Oleksy, A.; Blanco, A. G.; Boer, R.; Usón, I.; Aymamí, J.; Rodger, A.; Hannon, M. J.; Coll, M. *Angew. Chem., Int. Ed.* **2006**, *45*, 1834−1838.

(6) (a) Isele, K.; Franz, P.; Ambrus, C.; Bernardinelli, G.; Decurtins, S.; Williams, A. F. *Inorg. Chem.* **2005**, *44*, 3896−3906. (b) Provent, C.; Hewage, S.; Brand, G.; Charbonnière, L. J.; Williams, A. F.; Bernardinelli, G. *Angew. Chem., Int. Ed.* **1997**, *36*, 1287−1289. (c) Provent, C.; Bernardinelli, G.; Williams, A. F.; Vulliermet, N. *Eur. J. Inorg. Chem.* **2001**, *8*, 1963−1967.

(7) (a) Fletcher, N. C.; Brown, R. T.; Doherty, A. P. *Inorg. Chem.* **2006**, *45*, 6132−6134. (b) Fletcher, N. C.; Keene, F. R.; Viebrock, H.; von Zelewsky, A. *Inorg. Chem.* **1997**, *36*, 1113−1121. (c) Fletcher, N. C. *J. Chem. Soc., Perkin Trans.* **2002**, *16*, 1831−1842. (d) Fletcher, N. C.; Nieuwenhuyzen, M.; Rainey, S. *J. Chem. Soc., Dalton Trans*. **2001**, *18*, 2641−2648.

(8) (a) Ansa Hortala, M.; Fabbrizzi, L.; Foti, F.; Licchelli, M.; Poggi, A.; Zema, M. *Inorg. Chem.* **2003**, *42*, 664−666. (b) Amendola, V.; Fabbrizzi, L.; Gianelli, L.; Maggi, C.; Mangano, C.; Pallavicini, P.; Zema, M. *Inorg. Chem.* **2001**, *40*, 3579−3587. (c) Amendola, V.; Fabbrizzi, L.; Mangano, C.; Pallavicini, P.; Roboli, E.; Zema, M. *Inorg. Chem.* **2000**, *39*, 5803−5806. (d) Amendola, V.; Fabbrizzi, L.; Mundum, E.; Pallavicini, P. *Dalton Trans.* **2003**, *5*, 773−774.

(9) (a) Constable, E. C.; Frantz, R.; Housecroft, C. E.; Lacour, J.; Mahmood, A. *Inorg. Chem.* **2004**, *43*, 4817−4819. (b) Constable, E. C.; Heirtzler, F.; Neuburger, M.; Zehnder, M. *J. Am. Chem. Soc.* **1997**, *119*, 5606−5617. (c) Constable, E. C.; Edwards, A. J.; Raithby, P. R.; Walker, J. V. *Angew. Chem., Int. Ed. Engl.* **1993**, *32*, 1465−1467. (d) Constable, E. C.; Figgemeier, E.; Hougen, I. A.; Housecroft, C. E.; Neuburger, M.; Schaffner, S.; Whall, L. A. *Dalton Trans.* **2005**, *7*, 1168−1175. (e) Chow, H. S.; Constable, E. C.; Housecroft, C. E.; Neuburger, M.; Schaffner, S. *Dalton Trans.* **2006**, *23*, 2881−2890.

(10) (a) Albrecht, M. *Chem. Rev.* **2001**, *101*, 3457−3498. (b) Albrecht, M.; Mirtschin, S.; de Groot, M.; Janser, I.; Runsink, J.; Raabe, G.; Kogej, M.; Schalley, C. A.; Frohlich, R. *J. Am. Chem. Soc.* **2005**, *127*, 10371−10387. (c) Albrecht, M.; Dehn, S.; Raabe, G.; Fröhlich, R. *Angew. Chem., Int. Ed.* **2005**, *44*, 6448−6451. (d) Albrecht, M.; Schmid, S.; deGroot, M.; Weis, P.; Fröhlich, R. *Chem. Commun.* **2003**, *20*, 2526−2527. (e) Albrecht, M.; Witt, K.; Röttele, H.; Fröhlich, R. *Chem. Commun.* **2001**, *15*, 1330−1331. (f) Albrecht, M.; Janser, A. I.; Fleischhauer, J.; Wang, Y.; Raabe, G.; Fröhlich, R. *Mendeleev Commun.* **2004**, *6*, 250−253.

(11) (a) Yoon, J.; Mirica, L. M.; Stack, T. D. P.; Solomon, E. I. *J. Am. Chem. Soc.* **2005**, *127*, 13680−13693. (b) Yoon, J.; Mirica, L. M.; Stack, T. D. P.; Solomon, E. I. *J. Am. Chem. Soc.* **2004**, *126*, 12586−12595. (c) Enemark, E. J.; Stack, T.; Daniel, P. *Angew. Chem., Int. Ed.* **1998**, *37*, 932−935. (d) Enemark, E. J.; Stack, T.; Daniel, P.; Masood, M. A. *Angew. Chem., Int. Ed.* **1998**, *37*, 928−932.

(12) (a) Yeh, R. M.; Raymond, K. N. *Inorg. Chem.* **2006**, *45*, 1130−1139. (b) Fiedler, D.; Leung, D. H.; Bergman, R. G.; Raymond, K. N. *J. Am. Chem. Soc.* **2004**, *126*, 3674−3675. (c) Yeh, R. M.; Ziegler, M.; Johnson, D. W.; Terpin, A. J.; Raymond, K. N. *Inorg. Chem.* **2001**, *40*, 2216−2217. (d) Caulder, D. L.; Raymond, K. N. *Acc. Chem. Res.* **1999**, *32*, 975−982. (e) Ziegler, M.; Davis, A. V.; Johnson, D. W.; Raymond, K. N. *Angew. Chem., Int. Ed.* **2003**, *42*, 665−668. (f) Terpin, A. J.; Ziegler, M.; Darren, M.; Johnson, W.; Raymond, K. N. *Angew. Chem., Int. Ed.* **2001**, *40*, 157−160.

(13) (a) Wood, T. E.; Ross, A. C.; Dalgleish, N. D.; Power, E. D.; Thompson, A.; Chen, X.; Okamoto, Y. *J. Org. Chem.* **2005**, *70*, 9967−9974. (b) Wood, T. E.; Dalgleish, N. D.; Power, E. D.; Thompson, A.; Chen, X.; Okamoto, Y. *J. Am. Chem. Soc.* **2005**, *127*, 5740−5741. (c) Zhang, Y.; Thompson, A.; Rettig, S. J.; Dolphin, D. *J. Am. Chem. Soc.* **1998**, *120*, 13537−13538. (d) Thompson, A.; Rettig, S. J.; Dolphin, D. *Chem. Commun.* **1999**, *7*, 631−632.

(14) Franceschi, F.; Guillemot, G.; Solari, E.; Floriani, C.; Re, N.; Birkedal, H.; Pattison, P. *Chem.*−*Eur. J.* **2001**, *7*, 1468−1478.

(15) (a) Reid, S. D.; Blake, A. J.; Wilson, C.; Love, J. B. *Inorg. Chem.* **2006**, *45*, 636−643. (b) Arnold, P. L.; Blake, A. J.; Wilson, C.; Love, J. B. *Inorg. Chem.* **2004**, *43*, 8206−8208. (c) Love, J. B.; Salyer, P. A.; Bailey, A. S.; Wilson, C.; Blake, A. J.; Davies, E. S.; Evans, D. J. *Chem. Commun.* **2003**, *12*, 1390−1391.

(16) (a) Halper, S. R.; Cohen, S. M. *Inorg. Chem.* **2005**, *44*, 4139−4141. (b) Halper, S. R.; Cohen, S. M. *Inorg. Chem.* **2005**, *44*, 486−488. (c) Halper, S. R.; Cohen, S. M. *Angew. Chem., Int. Ed.* **2004**, *43*, 2385−2388.

(17) (a) Wu, Z.; Chen, Q.; Xiong, S.; Xin, B.; Zhao, Z.; Jiang, L.; Ma, J. S. *Angrew. Chem., Int. Ed.* **2003**, *42*, 3271−3274. (b) Yang, L.; Chen, Q.; Ma, J. S. *Tetrahedron* **2003**, *59*, 10037−10041. (c) Yang, L.; Shan, X.; Chen, Q.; Wang, Z.; Ma, J. S. *Eur. J. Inorg. Chem.* **2004**, *7*, 1474−1477. (d) Yang, L.; Chen, Q.; Li, Y.; Xiong, S.; Li, G.; Ma, J. S. *Eur. J. Inorg. Chem.* **2004**, *7*, 1478−1485. (e) Zhang, G.; Yang, G.; Chen, Q.; Ma, J. S. *Cryst. Growth Des.* **2005**, *5*, 661−666. (f) Zhang, G.; Yang, G.; Zhu, L.; Chen, Q.; Ma, J. S. *Sens. Actuators B* **2004**, *99*, 511−515. (g) Wu, Z.; Chen, Q.; Yang, G.; Xiao, C.; Liu, J.; Yang, S.; Ma, J. S. *Sens. Actuators B* **2006**, *114*, 995−1000. (h) Zhang, G.; Yang, G.; Ma, J. S. *New Development in Organometallic Chemistry Research*; Cato, M. A., Ed.; Nova Science Publishers, Inc.: New York, 2006; Chapter 3, pp 63−90.

(18) Wu, Z.; Zhang, Y.; Ma, J. S.; Yang, G. *Inorg. Chem.* **2006**, *45*, 3140−3142.

gravimetric (TG) curve in the range of 50−200 °C was performed on a Perkin-Elmer TGA7 at a heating rate of 20 K min^{-1}. Samples for C, H, and N analysis were dried under vacuum, and the analysis was performed with a Carlo Erba 1106 instrument. The electrospray ionization mass spectroscopy measurements were carried out with a Bruker APEX II instrument. ^{1}H NMR spectra were recorded with a Bruker Avance dpx 400 MHz instrument using tetramethylsilane (TMS) as the internal standard.

The CD spectra in the solution and solid state were recorded with a Jasco J-810 dichrograph. For the solid-state CD measurements, crystalline samples were ground to a fine powder with potassium bromide (KBr) and compressed into transparent disks with a thickness of ∼0.8 mm. The freshly prepared KBr disks were rotated around the optical axis, and the CD recordings were made for several positions in order to check the reproducibility of the spectra.

The UV−visible spectra were recorded on a Perkin-Elmer lamda 35 UV−visible spectrometer. The second-order NLO intensity was approximately estimated by measuring a powder sample. A pulsed Q-switched Nd:YAG laser at a wavelength of 1064 nm was used as the excitation source; the backscattered second-harmonic-generation (SHG) light was passed through a filter that transmits only 532 nm radiation. The magnetic properties are measured on a MPMS-XL-5 (Quantum Design). We have optimized the structures of H_2L^R and H_2L^S with the AM1[19] method implemented in the *Gaussian 03* quantum chemical program package.

Synthesis of (*R*,*R*)- and (*S*,*S*)-Bis(pyrrol-2-ylmethyleneamine)-cyclohexanes $H_2(L^R)$ and $H_2(L^S)$. Pyrrole-2-carbaldehyde (1.9 g, 20 mmol) and either (*R*,*R*)-(+)- or (*S*,*S*)-(−)-diaminocyclohexane (1.14 g, 10 mmol) were dissolved in ethanol (20 mL). The mixture was stirred for a while, and then a few drops of glacial acetic acid was added. After a few seconds, a white precipitate was observed. After about 30 min, the precipitate obtained from filtration was washed with CH_3OH, dried in vacuum, and crystallized from CH_2Cl_2/CH_3OH. Yield: 60.7%. Mp: 203.8 °C (dec). MALDI-TOF MS: *m*/*z* 269.3 ($M + H^+$). FT-IR (KBr pellets): ν 3066, 2855, 1443, 1364, 1142, 1026, 741 cm^{-1}. ^{1}H NMR (300 MHz, $CDCl_3$, 25 °C, TMS): δ 7.76 (s, 2H, imine H), 7.84 (s, 2H, pyrrole H), 6.39 (d, 2H, pyrrole H), 6.20 (t, 2H, pyrrole H), 3.12 (q, 2H, cyclohexane H), 2.21 (m, 2H, cyclohexane H), 1.78 (4H, cyclohexane H), 1.58 (m, 2H, cyclohexane H), 1.40 (m, 2H, cyclohexane H). Anal. Calcd for $C_{16}H_{20}N_4$ (268.36): C, 71.61; H, 7.51; N, 20.88. Found: C, 71.02; H, 7.39; N, 20.69.

General Procedure for the Synthesis of Metal Complexes of (*R*,*R*)- and (*S*,*S*)-Bis(pyrrol-2-ylmethyleneamine)cyclohexanes. A solution of metal(II) acetate dihydrate, $[M(CH_3CO_2)_2 \cdot xH_2O]$ (M = Ni, Cu, Zn; 1 mmol), in methanol (20 mL) was added to a solution of H_2L^R or H_2L^S (1 mmol) in methanol (10 mL). After 1.5 h, the precipitates, $[M(L^{R,S})]$ or $[M_2(L^{R,S})_2]$ (M = Ni, Cu, Zn), were collected by suction filtration and washed with methanol. Crystals suitable for X-ray analysis were obtained by recrystallization from CH_2Cl_2/CH_3OH.

Characterization of $[Ni^{II}(L^R)]$ and $[Ni^{II}(L^S)]$. Yield: 67.0%. Mp: 225−230 °C (dec). MALDI-TOF MS: *m*/*z* 324.3 (M^+). FT-IR (KBr pellets): ν 2932, 1634, 1578, 1384, 1296, 1034, 731 cm^{-1}. ^{1}H NMR (400 MHz, $CDCl_3$, 25 °C, TMS): δ 7.18 (s, 4H, imine H), 6.79 (s, 4H, pyrrole H), 6.57 (d, 4H, pyrrole H), 6.11 (s, 4H, pyrrole H), 3.35 (s, 4H, cyclohexane H), 2.21 (s, 4H, cyclohexane H), 1.82 (s, 4H, cyclohexane H), 1.27 (d, 8H, cyclohexane H). Anal. Calcd for $C_{16}H_{18}N_4Ni$ (325.05): C, 59.12; H, 5.58; N, 17.24. Found: C, 58.97; H, 5.63; N, 17.17.

Characterization of $[Cu^{II}(L^R)]$ and $[Cu^{II}(L^S)]$. Yield: 65−75%. Mp: 230 °C (dec). MALDI-TOF MS: *m*/*z* 329.3 (M^+). δ 7.17 (s, 4H, imine H), 6.79 (s, 4H, pyrrole H), 6.57 (d, 4H, pyrrole H), 6.12 (s, 4H, pyrrole H), 3.33 (s, 4H, cyclohexane H), 2.22 (s, 4H, cyclohexane H), 1.82 (s 4H, cyclohexane H), 1.27 (d, 8H, cyclohexane H). FT-IR (KBr pellets): ν 2931, 2360, 1601, 1292, 1030, 814, 737 cm^{-1}. Anal. Calcd for $C_{16}H_{18}N_4Cu$ (329.88): C, 58.25; H, 5.50; N, 16.98. Found: C, 58.35; H, 5.53; N, 16.80.

Characterization of $[Zn^{II}_2(L^R)_2]$ and $[Zn^{II}_2(L^S)_2]$. Yield: 75%. Mp: 225−230 °C (dec). MALDI-TOF MS: *m*/*z* 662.4 (M^+). FT-IR (KBr pellets): ν 2931, 1579, 1441, 1384, 1311, 1033, 748 cm^{-1}. ^{1}H NMR (400 MHz, $CDCl_3$, 25 °C, TMS): δ 7.30 (s, 4H, imine H), 7.02 (s, 4H, pyrrole H), 6.74 (d, 4H, pyrrole H), 6.40 (q, 4H), 2.54 (d, 4H, cyclohexane H), 1.61 (d, 8H, cyclohexane H), 18 (m, 8H, cyclohexane H). Anal. Calcd for $C_{32}H_{36}N_8Zn_2$ (663.43): C, 57.93; H, 5.47; N, 16.89. Found: C, 57.97; H, 5.60; N, 16.55.

X-ray Crystallography. Crystals suitable for X-ray diffraction (XRD) studies were obtained as described above. XRD measurements were performed by using a Rigaku X-ray diffractometer (D/max-2400) with an X-ray source of Cu Kα (l = 1.5406 Å) at 40 kV and 120 mA, at a scan rate of 0.028 (2θ) per 0.12 s. Crystal structures were solved by direct methods and refined with a full-matrix least-squares technique using the *SHELXS-97* and *SHELXL-97* programs.[20] Anisotropic thermal parameters were assigned to all non-H atoms. Analytical expressions of neutral-atom scattering factors were employed. Accurate unit cell parameters were determined by a least-squares fit of 2θ values, measured for 200 strong reflections, and intensity data sets were measured on a Bruker Smart 1000 CCD or Rigarku R-AXIS Rapid IP diffractometer with Mo Kα radiation (λ = 0.710 73 Å) at room temperature. The intensities were corrected for Lorentz and polarization effects, but no corrections for extinction were made. The H atoms were added theoretically and treated as riding on the concerned atoms. Crystallographic data and experimental details for structure analyses are summarized in Table 1. CCDC 299486, 299487, and 299574−299579, containing the supplementary crystallographic data for this paper, can be obtained free of charge at www.ccdc.cam.ac.uk/conts/retrieving.html or from the Cambridge Crystallographic Data Centre, 12 Union Road, Cambridge CB21EZ, U.K. [fax, (+44)-1223/ 336-033; e-mail, deposit@ccdc.cam.ac.uk].

Results and Discussion

The chiral ligands $[H_2(L^R)]$ and $[H_2(L^S)]$ were prepared in high yields by the condensation of the *R*,*R* and *S*,*S* enantiomers of the 1,2-diaminecyclohexane spacer with 2 equiv of pyrrole-2-carbaldehyde in ethanol. The reaction of $[H_2(L^{R,S})]$ with nickel(II), copper(II), or zinc(II) hydrated acetate in methanol leads to $[Ni^{II}(L^{R,S})]$, $[Cu^{II}(L^{R,S})]$, or $[Zn^{II}_2(L^{R,S})_2]$ complexes, respectively, in excellent yields.[17b−d] The ligand and complexes, isolated as white $[H_2(L^{R,S})]$, red $[Ni^{II}(L^{R,S})]$, black $[Cu^{II}(L^{R,S})]$, and white $[Zn^{II}_2(L^{R,S})_2]$ powders, are soluble in most common organic solvents. The ^{1}H NMR spectra of the free ligand $[H_2(L^{R,S})]$ and their metal complexes in $CDCl_3$ can be fully assigned, which suggests that they exist as single species in solution. No signal of the NH proton was observed in metal complexes, which is in agreement with deprotonation of the Schiff bases.[17] Moreover, metal complexes have upfield shifts for most of the protons as compared with free ligands. The ^{1}H NMR data also suggest

(19) Dewar, M.; Thiel, W. *J. Am. Chem. Soc.* **1977**, *99*, 4499−4500.

(20) Sheldrick, G. M. *SHELXL-97, Program for Crystal Structure Refinement*; University of Göttingen: Göttingen, Germany, 1997.

Table 1. Crystallographic Data and Structure Refinement Summary

	$H_2L^{R,S}$	$Ni^{II}L^{R,S}$	$Cu^{II}L^{R,S}$	$Zn^{II}L^{R,S}$
empirical formula	$C_{16}H_{20}N_4$	$C_{16}H_{18}N_4Ni$	$C_{16}H_{18}N_4Cu$	$C_{32}H_{36}N_8Zn_2$
mol wt	268.36	325.05	329.88	663.43
cryst syst	monoclinic	triclinic	monoclinic	orthorhombic
space group	$P2_12_12$	$P2_1$	$P2_1$	$C2$
a (Å)	18.897(4)	8.3594(17)	8.2254(16)	19.370(3)
b (Å)	8.8391(18)	11.299(2)	11.116(2)	10.1918(15)
c (Å)	9.4261(19)	16.710(3)	16.753(3)	16.074(2)
α (deg)	90	90	90	90
β (deg)	90	111.72(5)	107.62(8)	111.(258)
γ (deg)	90	90	90	90
D_{calcd} (g cm^{-3})	1.165	1.425	1.470	1.389
V (Å^3)	1530.6(5)	1515.6(5)	1490.1(5)	3173.3(8)
Z	4	4	4	4
abs coeff (mm^{-1})	0.072	1.278	1.464	1.546
F(000)	576	680	684	1376
cryst size (mm^3)	0.80 × 0.35 × 0.28	0.80 × 0.10 × 0.06	0.82 × 0.25 × 0.19	0.32 × 0.22 × 0.12
h	−22/24	1.24/27.48	−9/10	−24/23
k	0/11	0/10	0/14	−12/10
l	−12/11	13/14	−21/21	−15/20
θ range	2.22 to 27.32	−21 to +21	2.22 to 27.43	2.10 to 26.37
R^a	0.0431	0.0641	0.0330	0.0326
wR^b	0.0574	0.1174	0.0466	0.0984
GOF	1.029	1.071	1.005	0.995
largest diff peak/hole (e Å^{-3})	0.210/−0.166	0.509/ −0.643	0.595/ −0.588	0.299/−0.332

that the conformations for all metal complexes in the solid state still remain in the solution.

1. Crystal Structures. A. Helical Polymers [(H_2L·H_2O)$_n$]. The X-ray crystal structure for [(H_2L^S·H_2O)$_n$] is shown in Figure 2 (Figure S1 in the Supporting Information for [(H_2L^R·H_2O)$_n$]). It can be seen from Figure 2a that the two ligand arms in [$H_2(L^S)$] are preorganized along a helical P handedness because of the reciprocal arrangement of the

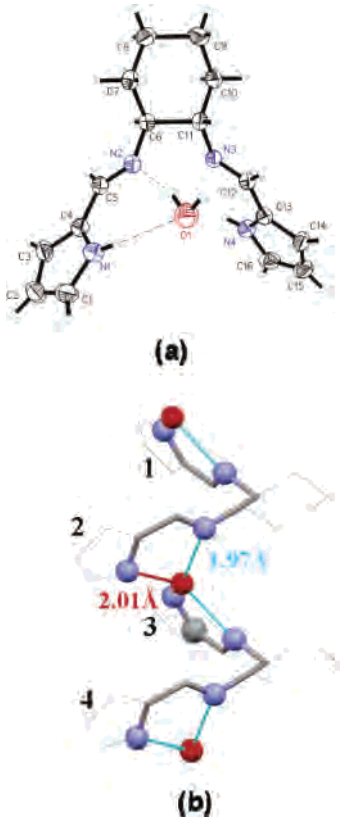

Figure 2. (a) ORTEP view of [$H_2(L^S)$·H_2O] with atomic numbering (30% thermal ellipsoid probability). (b) Ball-and-stick scheme of [($H_2(L^S)$·H_2O)$_n$]. Some atoms were omitted for clarity.

C−N_{imine} bonds in the semirigid (*S*,*S*)-1,2-cyclohexyl moiety ([$H_2(L^S)$]), which predetermines a M handedness.[8c] The angle between the two short axes of subunits is dependent on the rotation along the C−N_{imine} bond. The single-crystal XRD structure in Figure 2a shows that the two subunits in the same ligand molecule point up and down, respectively, consistent with the energy-optimized ligand conformation (see Figure S2 in the Supporting Information).

It can be seen from Figure 2b that linkage of parallel H_2L^S molecules by H_2O molecules results in a polymeric [(H_2L^S·H_2O)$_n$] chain. The pointing-down arm in the upper [$H_2(L^S)$] is connected to the pointing-up arm in the lower [$H_2(L^S)$] by one H_2O molecule, through two NH···O (2.01 Å, red line connections) and two N···HO (1.97 Å, blue line connections) hydrogen bonds. Interestingly, these two chromophores also arrange in a P right-handedness with respect to the linkage H_2O molecule[8c] (see Figure 2c). This leads [(H_2L^S·H_2O)$_n$] to form an infinite P right-handedness helix along the crystal *b* axis with a pitch = 5.59 Å. Furthermore, the homochiral infinite 1D helicates self-assemble into 2D sheets by C8H···*C*1 or C9H···*C*16 (2.87 Å) contacts in the α plane (see Figure S3 in the Supporting Information), and the final 3D structure can be considered as the stacking of the 2D sheets. The TG analysis reveals that H_2O molecules in the lattice started loss at about 75 °C and completed at about 100 °C, which indicates that H_2O molecules in the lattice are not very stabilized (see Figure S4 in the Supporting Information).

B. $Ni^{II}L$ and $Cu^{II}L$. The single-crystal analysis performed on the $Ni^{II}L$ and $Cu^{II}L$ complexes reveals that both of them display mononuclear single helicates.[17d] Part a and b of Figure 3 present the ORTEP drawings for [$Ni^{II}(L^S)$] and [Cu^{II}-(L^S)], respectively (see Figure S5 in the Supporting Information for [$Ni^{II}(L^R)$] and [$Cu^{II}(L^R)$]). The Ni^{II} and Cu^{II} centers demonstrate a distorted square-planar geometry in the complexes, upon tetracoordination to four N atoms from two arms in the same ligand. The dihedral angles, which are

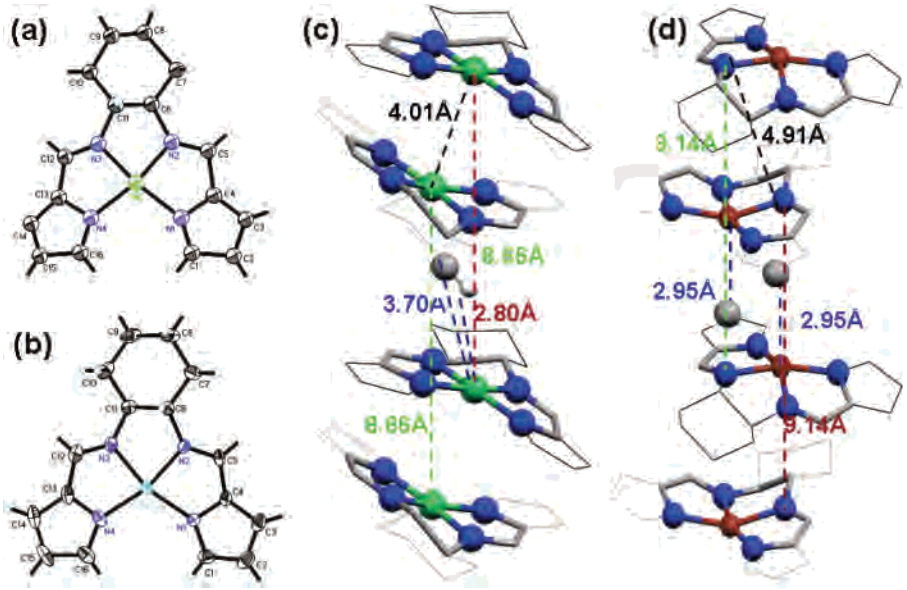

Figure 3. ORTEP views of the complexes Ni(L^S) (a) and Cu(L^S) (b) with atomic numbering (30% thermal ellipsoid probability). Ball-and-stick views of the Ni(L^S) (c) and Cu(L^S) (d) packings. Some atoms were omitted for clarity.

Table 2. Selected Bond Lengths (Å) and Bond Angles (deg) for Complexes NiL, CuL, and Zn_2L_2

covalent bonds		dative bonds	
bond	value	bond	value
	H_2L		
N1−H1−O1	2.795	N2−H2−O1	2.879
N3−H3−O1	2.795	N4−H4−O1	2.879
	CuL		
Cu1−N1	1.969	Cu1−N2	1.959
Cu1−N3	1.974	Cu1−N4	1.967
	NiL		
Ni1−N1	1.846	Ni1−N2	1.877
Ni1−N3	1.866	Ni1−N4	1.891
	Zn_2L_2		
Zn1−N5	1.955	Zn1−N6	2.070
Zn1−N8	1.978	Zn1−N7	2.055
Zn2−N2	1.955	Zn2−N1	2.070
Zn2−N3	1.976	Zn2−N4	2.055

Table 3. Selected Bond Angles (deg) for Complexes NiL, CuL, and Zn_2L_2

	H_2L		
N4−O1−N1	144.87	N1−O1−N2	62.04
N2−O1−N3	62.04	N3−O1−N4	144.87
	CuL		
N4−Cu1−N1	113.72	N1−Cu1−N2	82.4
N2−Cu1−N3	79.92	N3−Cu1−N4	82.6
	NiL		
N4−Ni1−N1	106.33	N1−Ni1−N2	84.07
N2−Ni1−N3	85.05	N3−Ni1−N4	84.75
	Zn_2L_2		
N4−Zn1−N1	85.19	N1−Zn1−N2	108.22
N2−Zn1−N3	84.78	N3−Zn1−N4	122.51
N4−Zn2−N1	85.19	N1−Zn2−N2	108.22
N2−Zn2−N3	84.78	N3−Zn2−N4	122.51

defined by the intersection of two planes at the metal ion center, are 8° for the Ni^{II} complex and 18° for the Cu^{II} complex, indicating that the Cu^{II} complex has more serious derivation from the square-planar coordination geometry. Selected bond lengths and angles of the two complexes are given in Tables 2 and 3. Moreover, the ligand $H_2(L^S)$ predetermined the P helix coordination and the ligand H_2-(L^R) predetermined the M helix coordination with Ni^{II} and Cu^{II}.[11d]

The crystal structures of $Ni^{II}L$ and $Cu^{II}L$ complexes also reveal interesting motifs through intermolecular weak interactions. Figure 3c depicts that, in a [$Ni^{II}(L^S)$] crystal, two helices, formed by reversibly oriented [$Ni^{II}(L^S)$] molecules as shown by the green and red dashed connections with a pitch = 8.66 Å, coil together, forming a 1D columnar structure along the crystal *b* axis. The crystal structure of [$Cu^{II}(L^S)$] also exhibits a similar 1D columnar structure along the crystal *a* axis, comprised of two helices with a pitch = 9.14 Å (see Figure 3d). Multiple metal contacts, CH···Ni 2.80 Å (HC···Ni 3.70 Å; see Figure 3c) and HC···Cu 2.95 Å (see Figure 3d), are also found in both crystals, probably responsible for the formation of columnar coil structures.[17d]

C. $Zn^{II}_2L_2$. The single-crystal X-ray analysis reveals that the reaction of H_2L with Zn^{II} gives rise to a double-stranded dinuclear structure of Zn_2L_2.[17a] Figure 4 shows the double-stranded helical geometry of [$Zn^{II}_2(L^S)_2$] (see Figure S6 in the Supporting Information for [$Zn^{II}_2(L^R)_2$]). The two subunits in the same (L^S) are bound to two different Zn^{II} ions, which additionally coordinate to another two subunits from another (L^S) ligand. The distance between the two Zn^{II} ions is 3.90 Å. The dihedral angle, which is defined by the intersection of two planes at the metal ion center, is 83°. The Zn^{II} ion and its two segments have an almost tetrahedral geometry, from which the bond angles and bond lengths have only a small deviation. Moreover, the ligand (L^S) predetermines the P helicates and the ligand (L^R) predetermines the M helicates.[11d]

The self-assembly of [$H_2(L^{R,S})$] with a H_2O molecule and metal ions Ni^{II}, Cu^{II}, and Zn^{II} gives rise to distinct molecular morphologies and crystal packing motifs. Homochiral and enantiopure infinite single-helical chains are formed by reaction with H_2O, while the mononuclear single-helical and

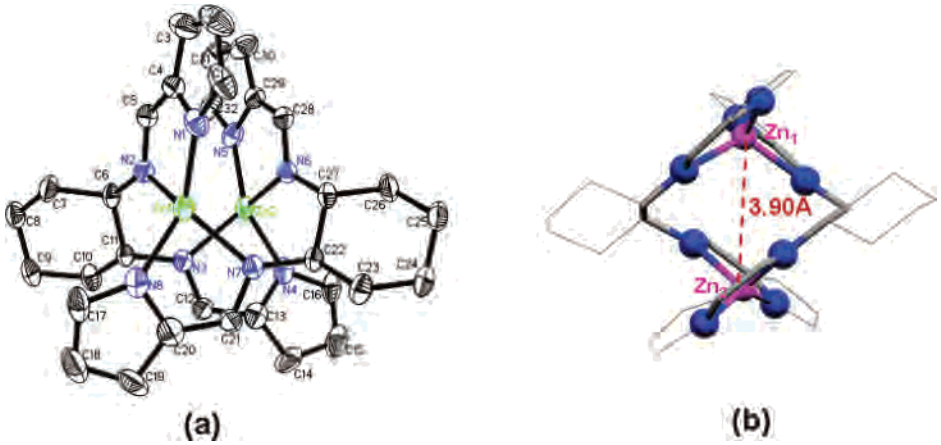

Figure 4. (a) ORTEP view of the complex $[Zn_2(L^S)_2]$ with atomic numbering (30% thermal ellipsoid probability). H atoms were omitted for clarity. (b)Ball-and-stick view of the packing of $[Zn_2(L^S)_2]$.

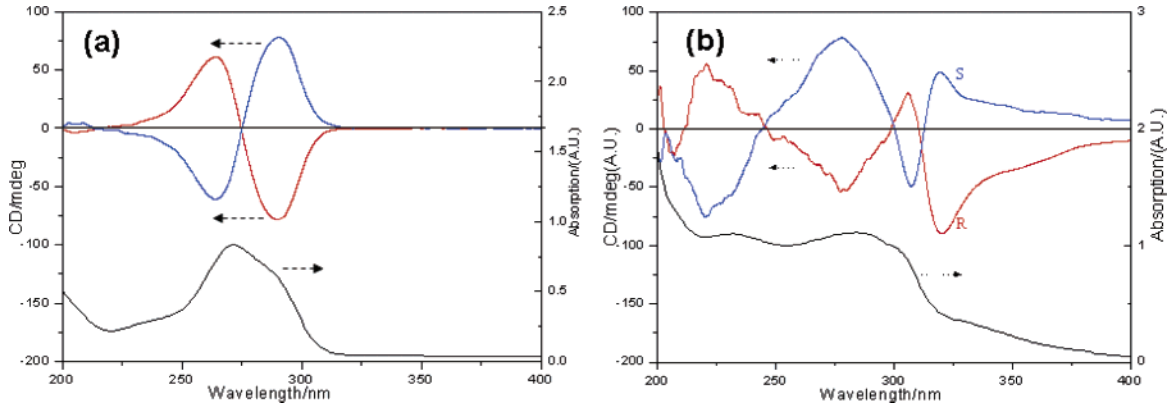

Figure 5. UV−visible (black) and CD spectra of (a) $H_2(L^{R,S})$ in CH_3CN solution and (b) $[(H_2(L^{R,S})\cdot H_2O)_n]$ in the solid state. The blue and red curves are CD spectra for *S* and *R* ligands, respectively.

double-stranded dinuclear helical metal complexes are obtained from coordination with metal cations Ni^{II}, Cu^{II}, and Zn^{II}, respectively. In any event, (L^S) predetermines a P right-handedness and (L^R) predetermines an M right-handedness.[8c,11d] This is considerably important in a biological system.[21] The packing patterns in the solid state might indeed be significant for the design and fabrication of useful functional material.[22] In order to investigate the influence of these structural changes on optical properties, we further measured the UV−visible absorption and CD spectra.

2. Optical Properties. A. $[(H_2L^S\cdot H_2O)_n]$. The UV−visible spectrum of $[H_2(L^{R,S})]$ in an acetonitrile solution (the black line in Figure 5a) shows the absorption bands at 250 and 280 nm, due to the $\pi-\pi^*$ and $n-\pi^*$ transitions, respectively. Note that the $\pi-\pi^*$ transition dipole moment is along the molecular long axis, while the $n-\pi^*$ transition dipole moment is along the molecular short axis. As mentioned above, the two subunits in the same ligand point up and down, respectively. This predicts a possible coupling between the $n-\pi^*$ transitions of two subunits. Indeed, the upper part of Figure 5 reveals that free ligands $[H_2(L^S)]$ and $[H_2(L^R)]$ in the solution present positive and negative exciton couplets in the region of the $n-\pi^*$ transition, i.e., mirror images, corresponding to P right-handedness (amplitude = +139) and M left-handedness (amplitude = −139), respectively. The Davydov splitting is $\Delta\lambda = 26.5$ nm at $\lambda = 277.25$ nm.

Figure 5b depicts the UV−visible absorption and CD spectra of $[(H_2(L^{R,S})\cdot H_2O)_n]$ in the solid state. The absorption of $[(H_2(L^{R,S})\cdot H_2O)_n]$ becomes broader than that of free ligands in the solution. The absorption edge extends to ~350 nm because of the increased intermolecular interactions in $[(H_2(L^{R,S})\cdot H_2O)_n]$, such as the interaction between chromophores 3 and 4 linked by H_2O in Figure 2b. Interestingly, we found that the solid-state CD spectra of $[(H_2(L^{R,S})\cdot H_2O)_n]$ display two bisignates at 250 and 310 nm, respectively (see the upper part of Figure 5b). In the free ligand, the exciton couplet at 277.25 nm results from the coupling of subunit pairs in the same molecule, for example, chromophore pairs (1, 2) or (3, 4) in Figure 2b. We ascribe the two CD bisignates at 250 and 310 nm of $[(H_2(L^{R,S})\cdot H_2O)_n]$ to intermolecular chromophore pair (2, 3) in Figure 2b. Further, the former might be due to the $\pi-\pi^*$ transitions, and the latter might be due to the $n-\pi^*$ transitions. The positive exciton couplet of $[(H_2(L^S)\cdot H_2O)_n]$ for a P handedness and the negative one of $[(H_2(L^R)\cdot H_2O)_n]$ for a M handedness are consistent with the single-crystal XRD analysis. According to a recent publication,[24] analysis of CD spectra of chiral polynuclear

(21) Dietrich-Buchecker, C. O.; Nierengarten, J.-F.; Sauvage, J.-p.; Armaroli, N.; Balzani, V.; DeCola, L. *J. Am. Chem. Soc.* **1993**, *115*, 11237.
(22) Binnemans, K.; Lodewyckx, K.; Donnio, B.; Guillon, D. *Chem.—Eur. J.* **2002**, *8*, 1101.

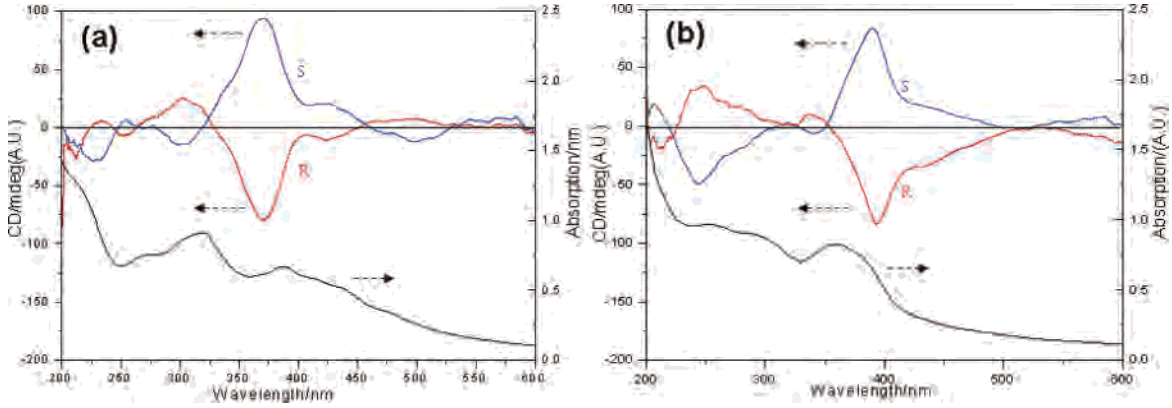

Figure 6. UV−visible (black) and CD spectra of (a) [$Ni^{II}(L^{R,S})$] and (b) [$Cu^{II}(L^{R,S})$] in the solid state. The blue and red curves are CD spectra for *S* and *R* ligands, respectively.

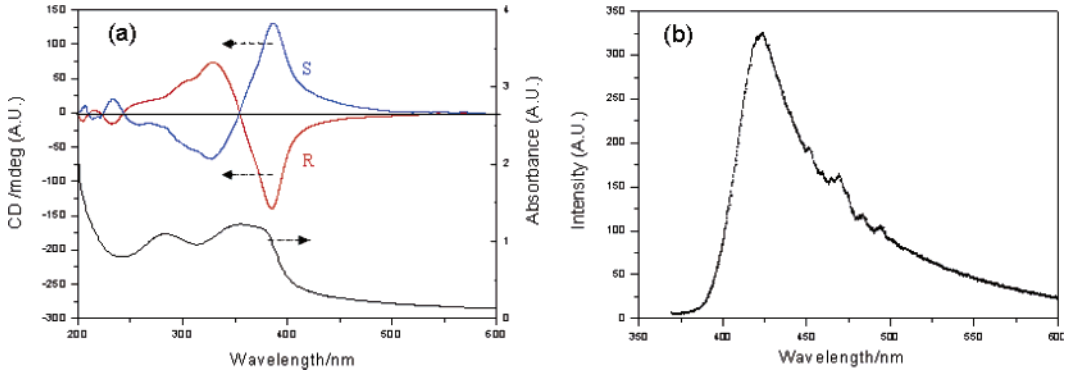

Figure 7. (a) UV−visible and CD and (b) emission spectra of the [$Zn^{II}_2(L^{R,S})_2$] complex in the solid state. In part a, the black curve is the absorption spectrum and the blue and red curves are CD spectra for *S* and *R* ligands, respectively. In part b, the excitation wavelength is 350 nm.

complexes must take internuclear coupling effects into account. In [$(H_2(L^S)\cdot H_2O)_n$], the Davydov splittings for the exciton couplet at 250 and 310 nm are $\Delta\lambda = 57.0$ and 13.2 nm, respectively. The broad CD signal between 200 and 300 nm might be a mixture of the couplings of chromophore pairs (1, 2) [or (3, 4)], (2, 3), and (1, 3) [or (2, 4)],[24c] shown in Figure 2b.

B. [$Ni^{II}(L^{R,S})$] and [$Cu^{II}(L^{R,S})$]. The UV−visible absorption and CD spectra of [$Ni^{II}(L^{R,S})$] complexes show very similar features in the solid state (see Figure 6a) and in solution (see Figure S7a in the Supporting Information), and similar cases are also found for [$Cu^{II}(L^{R,S})$] (see Figures 6a and S7b in the Supporting Information) and [$Zn^{II}_2(L^{R,S})_2$] (see Figures 7 and S7c in the Supporting Information) complexes. This further confirms that the basic unit for metal complexes is the same in solution as it is in the solid state.

It can be seen from Figure 6a that the $\pi-\pi^*$ and $n-\pi^*$ transitions in the [$Ni^{II}(L^{R,S})$] complex are shifted to 270 and 315 nm upon coordination. The broad absorption bands with a maximum at 385 nm are assigned to the metal-to-ligand charge transfer (MLCT) of Ni^{II} to $L^{R,S}$ transtions. The CD spectrum of the [$Ni^{II}(L^S)$] complex (see the blue line in Figure 6a) presents a mixture of a positive Cotton effect (CE) in the MLCT region and a positive exciton couplet in the $n-\pi^*$ region, consistent with the XRD analysis for a P right-handedness. However, the $n-\pi^*$ exciton coupling in the [Ni^{II}-$(L^{R,S})$] complex is weaker than that in the free ligand, as a result of the near-square-planar coordination geometry in [$Ni^{II}(L^{R,S})$].

Similar to [$Ni^{II}(L^{R,S})$] complexes, [$Cu^{II}(L^{R,S})$] complexes also present absorption bands at 255, 300, and 360 nm for the $\pi-\pi^*$ and $n-\pi^*$ transitions and the MLCT transition, respectively (see the black line in Figure 6b). All wavelengths in [$Cu^{II}(L^{R,S})$] complexes are a little blue-shifted from those in [$Ni^{II}(L^{R,S})$] complexes because the former has more serious derivation from the square-planar coordination geometry than the latter does. The CD spectrum of the [$Cu^{II}(L^{R,S})$] complex (see the blue line in Figure 6b) presents a positive CE in the Cu^{II} MLCT region and, furthermore, a negative CE in the $n-\pi^*$ and $\pi-\pi^*$ regions, which is not found in the [Ni^{II}-$(L^{R,S})$] complex.

C. [$Zn^{II}_2(L^{R,S})_2$]. The UV−visible spectrum of the [Zn^{II}_2-$(L^{R,S})_2$] complex (see the black line in Figure 7a) shows absorption bands at 280 and 354 nm, which are assigned to $n-\pi^*$ and Zn^{II} MLCT transitions, respectively. The CD (see the upper part in Figure 7a) reveals a strong bisignate CD in the region of the Zn^{II} MLCT transition.[17a,b,25] As mentioned

(23) Weber, J. H. *Inorg. Chem.* **1967**, *6*, 258−262.
(24) (a) Telfer, S. G.; Tajima, N.; Kuroda, R.; Cantuel, M.; Piguet, C. *Inorg. Chem.* **2004**, *43*, 5302−5310. (b) Telfer, S. G.; Sato, T.; Kuroda, R.; Lefebvre, J.; Leznoff, D. B. *Inorg. Chem.* **2004**, *43*, 421−429. (c) Telfer, S. G.; Tajima, N.; Kuroda, R. *J. Am. Chem. Soc.* **2004**, *126*, 1408−1418. (d) Telfer, S. G.; Sato, T.; Harada, T.; Kuroda, R.; Lefebvre, J.; Leznoff, D. B. *Inorg. Chem.* **2004**, *43*, 6168−6176. (e) Telfer, S. G.; Kuroda, R.; Sato, T. *Chem. Common.* **2003**, *9*, 1064−1065.
(25) Lever, A. B. P. *Inorganic Electronic Spectroscopy*, 2nd ed.; Elsevier: Amsterdam, The Netherlands, 1984; p 535.

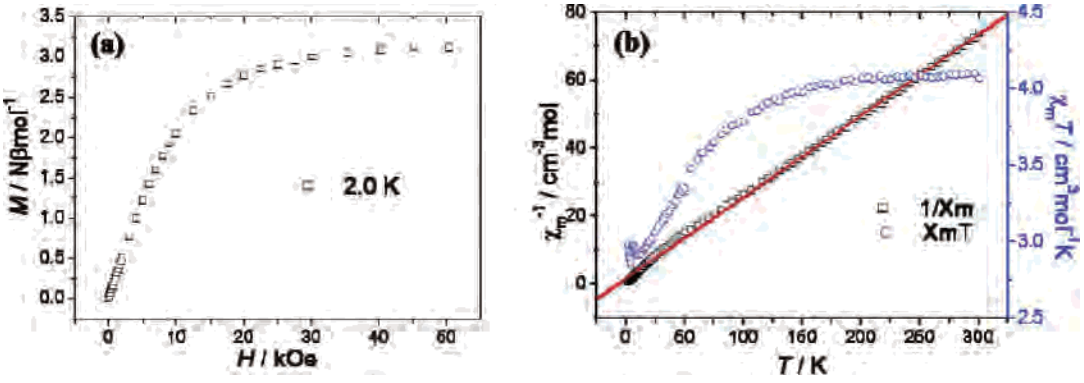

Figure 8. (a) Field dependence of M of [Cu($L^{R,S}$)] at 2.0 K. (b) Temperature dependence of $\chi_M T$ and χ_M^{-1} of [Cu($L^{R,S}$)] at a 10 kOe field. The red solid line represents the best fit to the Curie−Weiss expression.

in the section 1C, the [$Zn^{II}_2(L^{R,S})_2$] complex forms a double-stranded dinuclear helicate. The two chromophores in the same ligand coordinated with Zn^{II} ions held ~83° apart, which exhibit a bisignal induced by the exciton coupling. Factually, the coordination geometry in the [$Zn^{II}_2(L^R)_2$] complex is quite similar to that in [(H_2L^R·H_2O)$_n$], adopting a tetrahedronal geometry. However, the metal bonds are much stronger than the hydrogen bonds. Therefore, the Davydov splitting in [$Zn^{II}_2(L^S)_2$], i.e., $\Delta\lambda = 59$ nm at $\lambda = 354$ nm, is larger than that in [(H_2L^R·H_2O)$_n$], i.e., $\Delta\lambda = 26.5$ nm at $\lambda = 277.25$ nm.

D. Fluorescence Properties. Though the fluorescence of the Ni^{II} and Cu^{II} complexes are quenched, [$Zn^{II}_2(L^{R,S})_2$] complexes have a strong blue emission (see Figure S8 in the Supporting Information) at 420 nm and a low-energy tail extending to about 550 nm (see Figure 7b), which is assigned to chelation-enhanced fluorescence emission according to our previous work.[17f,g] Further, the fluorescence of this chiral complex is expected to exhibit a circularly polarized emission.[24,26] Utilization of the [$Zn^{II}_2(L^{R,S})_2$] complexes as potential circularly polarized fluorescence materials or luminescence materials is currently under investigation in this laboratory.

E. Second-Order NLO Properties. Because all of the complexes are acentric, they may be NLO-active.[27,28] The simple computational models of these complexes provide meaningful insight into the trends of molecular nonlinearity and suggest a convenient approach to the design of the complex for SHG application. The β values of these complexes are listed in Table 4, indicating that all of the four complexes have moderate hyperpolarizabilities. We also have performed quasi-Kurtz SHG measurements on microcrystal samples to confirm their acentricity as well as to evaluate their potential application as second-order NLO materials. Primary experimental results reveal that two, H_2L and $Zn^{II}_2L_2$, of the four compounds have moderate SHG efficiencies (Table 4). Both compounds exhibit excellent thermal stability and optical transparency, which make them potential candidates for practical applications.

Table 4. Static Hyperpolarizabilities of the Ligand and Ligand/Metal Complexes by the AM1 Calculations[a]

compound	$\beta/10^{-30}$ esu	SHG/U[b]
ligand	9.29	>urea
Ni^{II} complex	9.91	
Cu^{II} complex	10.07	
Zn^{II} complex	2.16	~urea

[a] The metal ions are replaced by point charges, and geometries are taken from the crystal structures with H atoms alone optimized in the AM1 method. [b] 1 U = SHG of urea.

F. Magnetism Properties. Primary experiments about the magnetism of [Cu($L^{R,S}$)] are conducted. The temperature dependence of the magnetic susceptibility χ_M of [Cu($L^{R,S}$)] was measured in a magnetic field of 1 kOe (Figure 8). The $\chi_M T$ value at room temperature is 4.09 $cm^3\ mol^{-1}$ K, which decreases smoothly upon cooling to ca. 10 K and then has a slight increase, followed by a decrease. The magnetic susceptibility in the range 20−300 K obeys the Curie−Weiss law with Curie constant $C = 4.175\ cm^3\ mol^{-1}$ K and a negative Weiss constant θ of −7.06 K, which indicates the presence of an antiferromagnet. Magnetism correlated with the chirality of the complexes may have potential application.[29]

Conclusion

In this paper, the enantiomerically pure bis-bidentate ligands of bis(pyrrol-2-ylmethyleneamine)cyclohexane [H_2-($L^{R,S}$)] are easily synthesized from condensation of the pure *R,R* and *S,S* enantiomers of the 1,2-diaminecyclohexane spacer with 2 equiv of pyrrole-2-carbaldehyde. The self-assembly of $H_2L^{R,S}$ with a H_2O molecule and metal ions Ni^{II},

(26) Petoud, S.; Muller, G.; Moore, E. G.; Xu, J.; Sokolnicki, J.; Riehl, J. P.; Le, U. N.; Cohen, S. M.; Raymond, K. N. *J. Am. Chem. Soc.* **2007**, *129*, 77−83.

(27) (a) Moulton, B.; Zaworoko, M. J. *Chem. Rev.* **2001**, *101*, 1629−1658. (b) Kesanli, B.; Lin, W. *Coord. Chem. Rev.* **2003**, *246*, 305−326. (c) Zhang, H.; Wang, X.; Zhang, K.; Teo, B. K. *Coord. Chem. Rev.* **1999**, *183*, 157−159. (d) Evans, O. R.; Lin, W. *Acc. Chem. Res.* **2002**, *35*, 511−522.

(28) (a) Anthony, S. P.; Basavaiah, K.; Radhakrishnan, T. P. *Cryst. Growth Des.* **2005**, *5*, 1663−1666. (b) Gangopadhyay, P.; Radhakrishnan, T. P. *Angew. Chem., Int. Ed.* **2001**, *40*, 2451−2455. (c) Philip Anthony, S.; Radhakrishnan, T. P. *Chem. Commun.* **2004**, *9*, 1058−1059.

(29) (a) Benelli, C.; Gatteschi, D. *Chem. Rev.* **2002**, *102*, 2369−2388. (b) Inoue, K.; Imai, H.; Ghalsasi, P. S.; Kikuchi, K.; Ohba, M.; Okawa, H.; Yakhmi, J. V. *Angew. Chem., Int. Ed.* **2001**, *40*, 4242−4245. (c) Andres, R.; Brissard, M.; Gruselle, M.; Train, C.; Vaissermann, J.; Malezieux, B.; Jamet, J.-P.; Verdaguer, M. *Inorg. Chem.* **2001**, *40*, 4633−4640. (d) Coronado, E.; Gomez-Garcia, C. J.; Nuez, A.; Romero, F. M.; Rusanov, E.; Stoeckli-Evans, H. *Inorg. Chem.* **2002**, *41*, 4615−4617. (e) Gao, E.-Q.; Bai, S.-Q.; Wang, Z.-M.; Yan, C.-H. *J. Am. Chem. Soc.* **2003**, *125*, 4984−4985.

Cu^{II}, and Zn^{II} gives rise to distinct molecular morphologies and crystal packing motifs: homochiral and enantiopure infinite single-helical polymeric chains of $[(H_2L^{R,S}\cdot H_2O)_n]$ via hydrogen bonds, mononuclear single helices of $[Ni^{II}(L^{R,S})]$ and $[Cu^{II}(L^{R,S})]$, and a double-stranded dinuclear helicate of $[Zn^{II}{}_2(L^{R,S})_2]$, respectively. The structures for all metal complexes in the solid state still remain in the solution. Remarkably, chiral ligands of $H_2(L^R)$ and $H_2(L^S)$ predetermine the chirality of the helical complexes, i.e., M left-handedness and P right-handedness, respectively. The structural changes of these complexes induced by different coordinators are also characterized by CD and absorption spectra in both the solid state and solution. Analysis of CD spectra, with aids of absolute determination of single-crystal XRD structures, reveals both intraligand and interligand chromophore couplings. For the potential applications of these chiral complexes, other experiments such as photoluminescence and NLO properties have also been investigated.

Acknowledgment. This work was supported by the National Natural Science Foundation of China (Grants 50221201, 90301010, and 90606004), the Chinese Academy of Sciences, and the National Research Fund for Fundamental Key Project 973 (2006CB806200, 2006CB932101).

Supporting Information Available: TG curves, XRD patterns, and additional crystallographic figures for the structural determination of all compounds. This material is available free of charge via the Internet at http://pubs.acs.org.

IC062316Z